Computational studies of swirl effects on instabilities and pollutions due to non-premixed turbulent combustion

Luthenda Gamany[1] , Taha Janan Mourad[2] and Agouzoul Mohamed[1]

[1] Equipe de Recherche et Développement : Modélisation et Multimédia Mécanique (ERD3M)
UFR : Modélisation et Calcul Informatique en Conception Mécanique (MCICM)
Ecole Mohammedia d'Ingénieurs – EMI, University Mohammed V Agdal (UM5A)
Postal address: Avenue Ibn Sina, B.P 765, Agdal, Rabat 10000, Morocco
[2] Laboratoire de Mécanique Procédés et Processus Industriels (LM2PI)
Ecole Normale Supérieure de l'Enseignement Technique – ENSET,
Postal address: Avenue de l'Armée Royale, Madinat Al Irfane 10100, B.P. 6207 Rabat-Instituts, Rabat 10000, Morocco

Abstract
Considerable effort is currently being extended by means of open CFD analysis to examine and fight against mechanisms responsible of combustion instabilities and environment pollution due to CO_2 and NO productions. To achieve that, the present paper suggests a system based on injection of a secondary air swirling flow in a non-premixed turbulent combustion chamber fed by fuel oil n°2. Computational studies are based on analysis of swirl intensity impact using OpenFOAM's solver named reactingFoam to compare the recommended system to a basic combustor of drying furnace. Data allowing discussions are temperatures and concentrations of unburned species and products of gas combustion calculated at transversal and longitudinal sections of the combustion chamber. The fact that results obtained reveal no risk of flashback or blowing phenomena, fast diminution of unburned products, significant thermal losses near walls, reduction of CO_2 production combined to a rise of NO formation pushes us to investigate more about the proposed apparatus.

Keywords: Coflow Non-premixed turbulent combustion OpenFOAM reactingFoam Swirling flow Swirl number

1. Introduction

The need for increased fuel consumption efficiency and environmental protection regulations are imposing stricter requirements on high intensity industrial combustion systems. In particular, the need to limit energy consumption costs, the restrictions on NO and soot emissions and the competitive placement in the market have encouraged the introduction of innovative solutions for better combustion control and the extrapolation of new concepts to practical designs. In non-premixed turbulent combustion area several efforts are made to accord experimental and numerical studies but still are insufficient compared to requirements becoming more and stricter. Gupta A. K. et al. [9] will be among the first to reveal (by means of experimental results) the important effects of swirl on promoting flame stability, increasing combustion efficiency and controlling emission of pollutants from combustion. Even if CFD (Computational Fluids Dynamics) analysis will later confirm this thesis through advanced modeling and simulation, the prediction of flames stabilized by swirling jet continues to be a research area under exploration. Due to the importance of this type of fluid flow, considerable investigations have been performed in this regard. Many projects were conducted to increase interaction between experimentalists and numerical analysts in order to reach good agreements between theory and realistic phenomena. Among these projects two references can be typically cited: CORIA (COmplexe de Recherche Interprofessionnel en Aérothermochimie) [5, 25] and TNF (the International workshop on measurement and computation of Turbulent Non-premixed Flames) [4]. To boost TNF researches, experimental simulations devices like PRECCINSTA [1] and TECFLAM [1, 11] swirl burners were developed but two limitations can be identified.

The first one concerns the nature of fuels used by PRECCINSTA and TECFLAM. These are more suitable for gas fuels (methane, natural gas, etc.) with direct applications in gas turbine combustors or in aircraft engines [18]. In our case, the fuel is a preheated liquid (fuel oil n°2) used in industrial drying furnaces [14]. According to CFD literature, it's less complicated to predict flames based on gaseous hydrocarbons than heavy oils [5, 16]. This difficulty comes a part from strong influence of high viscosities on turbulence and combustion phenomena. And this is clearly seen during modeling and simulation of instabilities and mixtures.

Another limitation is about PRECCINSTA and TECFLAM basic configurations. In most cases swirl jet is involved in primary air flows [1, 13] while this one is located in secondary air flows (Fig.4). In these kinds of situations the size of confinement plays an important role in the aerodynamics of flame [5].

In addition, the problem here is complicated by 3D assumption according to the complexity of systems and phenomena.

Despite all this, giving predictions that can satisfy industrial requirements (performance and security of systems), standards of environment protection (fight against pollution) and computational efficiency (need of precision, speed and robustness) still be a topical challenge in CFD.

2. Description of the problem

2.1. Geometry

In this study, the combustion chamber geometry is a typical case of those used in industrial drying furnaces (Fig. 1) [14]. To obtain a non-premixed turbulent flame, the fuel oil n°2 is injected through the internal tube of the burner after being preheated and sprayed. At the same time, primary air at ambient temperature is introduced through the annular space. It is assumed that the two considered flows are coaxial. Finally, secondary air is introduced through 24 circular orifices on the edges of the front of our firebox (Fig. 1). To obtain a swirling flow (Fig. 3), system of axial and tangential injection of air [5] is used by mean of exhaust fans [14].

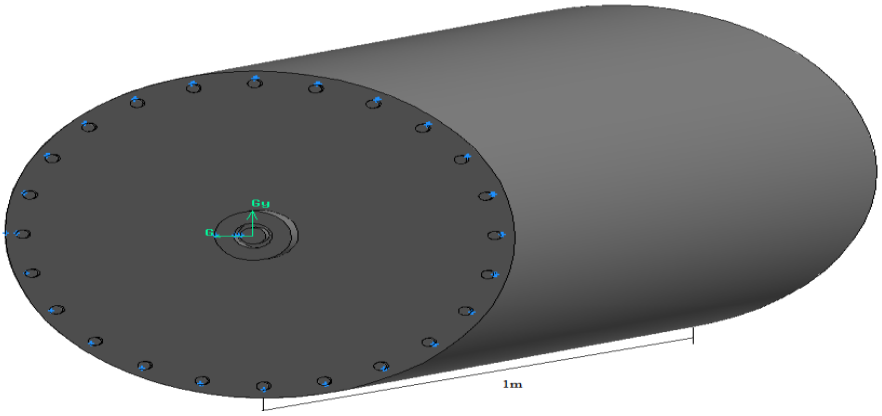

Fig. 1: Combustion chamber

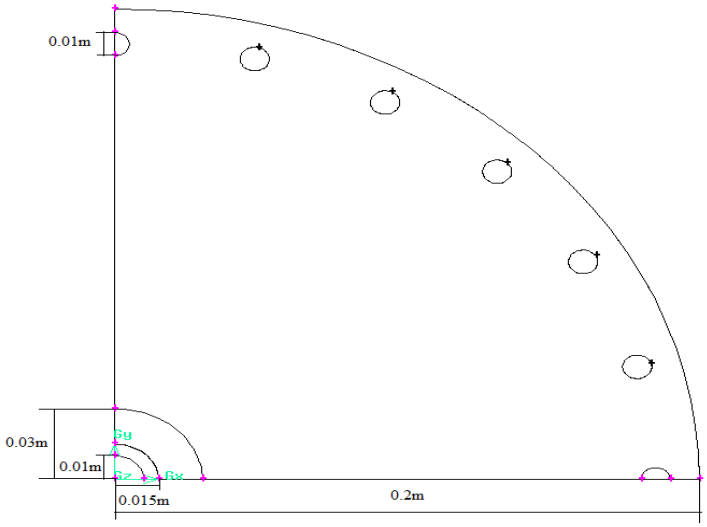

Fig. 2: Face measures

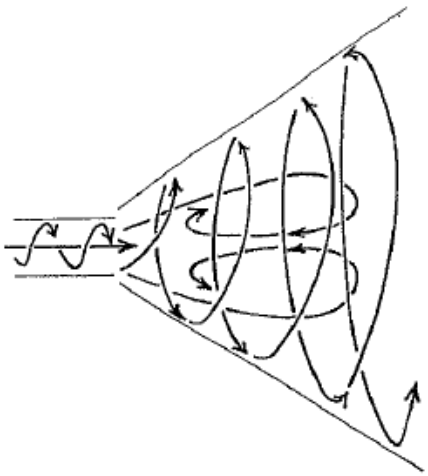

Fig. 3: Swirl Flow with Internal Zone Recirculation

2.2. Boundary conditions

Experimental data obtained from measurements [14] are used in order to approach realistic situation. Entrance conditions are related to the flow rate and the temperature given from the burner exit. The inlet velocities of fuel and primary air are respectively 2.34m/s and 15m/s while their respective temperatures are 120°C and 17°C. The outlet conditions are related to the pressure. The temperature of the nozzle was fixed to 980°C which is the limit of security imposed. According to the secondary air, the inlet velocity is a rotating profile field whose variation depends on the ratio of flow rates injection. About the walls, they are supposed to be adiabatic.

3. Mathematical formulation

3.1. Swirling Flow

Commonly, it is possible to obtain a swirling flow either by using an insert inside the nozzle or by mixing two air flows. The last study on a swirling impinging jet is due to Ward and Mahmood [20]. The swirling jet designed by Ward and Mahmood, which is based on the concept of mixing an axial air flow with a tangential one, is characterized by a radial distribution of the local convective heat transfer, which, respect to the circular jet, is slightly more uniform with a significantly lower heat transfer rate.

3.1.1. Swirl number (S) [9]

The standard method used to stabilize flames in current lean premixed combustors is based on swirling injection. Combustion is established around a hot gas kernel formed by the swirling flow. The lower pressure region created in the central region by swirl generates an internal recirculation zone of burnt gases anchoring the flame. This region designated as the inner recirculation zone (IRZ) is associated with the vortex breakdown process which takes place in swirling flows [3, 4]. The intensity of a swirling flow is given by a dimensionless number *S* called swirl number. This quantity establishes the relationship between the axial flux of kinetic momentum and the axial flux of axial momentum.

$$S = G_\theta / RG_x \tag{1}$$

G_θ can also be seen as the flux of tangential momentum and G_x the flux of momentum following the direction of propagation. After developing the previous expression, *S* becomes:

$$S = \frac{\int_0^R \rho\left(\overline{uw} + \overline{u'w'}\right) r^2 dr}{R\int_0^R \rho\left(u^2 + \frac{\left(\overline{w}^2 - w_{\max}^2\right)}{2}\right) r dr} \tag{2}$$

Where *R* is the radius of the injector tube and $\vec{V}(u,v,w)$ the velocity decomposed into mean and fluctuating values: $u = \overline{u} + u'$, $v = \overline{v} + v'$, $w = \overline{w} + w'$

3.1.2. Equation of conservation of momentum for a swirling flow [8]

As it has been already mentioned on chap. 2. 2, the entrance of secondary air is characterized by a rotating velocity field. The absence of circumferential gradients in the swirling flow led us to consider the assumption of an axisymmetric configuration in order to establish the initial solution. We have now a 2D model with prediction of the circumferential velocity. Its equation of conservation of tangential momentum is:

$$\frac{\partial}{\partial t}(\rho w) + \frac{1}{r}\frac{\partial}{\partial x}(r\rho uw) + \frac{1}{r}\frac{\partial}{\partial r}(r\rho vw) = \frac{1}{r}\frac{\partial}{\partial x}\left[r\mu\frac{\partial w}{\partial x}\right] + \frac{1}{r^2}\frac{\partial}{\partial r}\left[r^3\mu\frac{\partial}{\partial r}\left(\frac{\partial w}{\partial r}\right)\right] - \rho\frac{vw}{r} \tag{3}$$

3.2. Equations of the combustion

This section presents governing equations of combustion flow in the furnace. Chemical reactions that can be modeled include liquid fuel combustion in which fuel vapor is generated via evaporation of liquid droplets and a combustion reaction occurs in the gas phase.

3.2.1. Governing equations in conservative form [1]

Equations of chemical species reacting flow in conservative form can be written as follows:

$$\frac{\partial \mathrm{w}}{\partial t} + \nabla \cdot \mathrm{F} = \mathrm{s} \tag{4}$$

Where $\mathrm{w} = (\rho u, \rho v \rho w, \rho E, \rho_k)^T$ with ρ the density, $\vec{\mathrm{V}} = (u,v,w)^T$ the vector velocity, E the total energy and $\rho_k = \rho Y_K$ with Y_K the mass fraction of K species. Flux tensor can be decomposed in two parts:

$$\mathrm{F} = \mathrm{F(w)}^{\mathrm{I}} + \mathrm{F(w,\nabla w)}^{\mathrm{V}} \tag{5}$$

Where $\mathrm{F(w)}^{\mathrm{I}}$ is non-viscous tensor and has 3 components:

$$f^{I}=\begin{pmatrix}\rho u^{2}+P\\ \rho uv\\ \rho uw\\ (\rho E+P)u\\ \rho_{K}u\end{pmatrix},\quad g^{I}=\begin{pmatrix}\rho uv\\ \rho u^{2}+P\\ \rho uw\\ (\rho E+P)v\\ \rho_{K}v\end{pmatrix},\quad h^{I}=\begin{pmatrix}\rho uw\\ \rho vw\\ \rho w^{2}+P\\ (\rho E+P)w\\ \rho_{K}w\end{pmatrix} \tag{6}$$

Where P is the hydrostatic pressure defined in perfect gas state equation.

$F(w,\nabla w)^{V}$ is viscous tensor and has 3 components:

$$f^{V}=\begin{pmatrix}-\tau_{xx}\\ -\tau_{xy}\\ -\tau_{xz}\\ -(u\tau_{xx}+v\tau_{xy}+w\tau_{xz})+q_{x}\\ J_{x,K}\end{pmatrix},g^{V}=\begin{pmatrix}-\tau_{xy}\\ -\tau_{yy}\\ -\tau_{yz}\\ -(u\tau_{xy}+v\tau_{yy}+w\tau_{yz})+q_{y}\\ J_{y,K}\end{pmatrix},h^{V}=\begin{pmatrix}-\tau_{xz}\\ -\tau_{yz}\\ -\tau_{zz}\\ -(u\tau_{xz}+v\tau_{yz}+w\tau_{zz})+q_{z}\\ J_{z,K}\end{pmatrix}$$

(7)

Stress tensor is defined as follows:

$$\tau_{ij}=2\mu\left(S_{ij}-\frac{1}{3}\delta_{ij}S_{ll}\right),i,j=1,3 \tag{8}$$

$$S_{ij}=\frac{1}{2}\left(\frac{\partial u_{j}}{\partial x_{i}}+\frac{\partial u_{i}}{\partial x_{j}}\right),i,j=1,3 \tag{9}$$

3.2.2. Equation of state of perfect gas

The mixture formed in the furnace is supposed to be mixture of perfect gas:

$$P=\rho\frac{R}{\overline{W}}T \tag{10}$$

$\overline{W}$ is the mixture molecular weight:

$$\frac{1}{\overline{W}}=\sum_{K=1}^{N}\frac{Y_{K}}{W_{K}} \tag{11}$$

R = 8.3143J/mol.K is the universal constant of perfect gas.

3.2.3. Equation of continuity

Conservation of total mass in multi species flow is satisfied by the following equations:

$$\sum_{K=1}^{N}Y_{K}V_{i}^{K}=0 \tag{12}$$

V_{i}^{K} represents the velocity component of diffusion of the species k in the i direction (i=1,2,3). The approximation of Hirschfelder-Curtis is used to express this velocity of diffusion:

$$X_{K}V_{i}^{K}=-D_{K}\frac{\partial X_{K}}{\partial x_{i}} \tag{13}$$

$$Y_{K}V_{i}^{K}=-D_{K}\frac{\overline{W_{K}}}{W}\frac{\partial X_{K}}{\partial x_{i}} \tag{14}$$

Where X_K are gradients of mole fractions.

3.2.4. Heat flux

The total heat flux q_i is the sum of 2 terms: the heat flux by conduction and the heat flux by diffusion of species.

$$q_{i}=-\lambda\frac{\partial T}{\partial x_{i}}+\sum_{K=1}^{N}J_{i,k}h_{S,K} \tag{15}$$

$$q_i = -\overbrace{\lambda\frac{\partial T}{\partial x_i}}^{\text{conduction}} \overbrace{-\rho\sum_{K=1}^{N}\left(D_K\frac{W_K}{\overline{W}}\frac{\partial X_K}{\partial x_i} - Y_K\sum_{K=1}^{N}D_K\frac{W_K}{\overline{W}}\frac{\partial X_K}{\partial x_i}\right)h_{S,K}}^{\text{Diffusion of species}} \quad (16)$$

4. Implementation in OpenFOAM

The choice of implementation in OpenFOAM as CFD code compared to the commercial counterparts, e.g. Fluent and Ansys CFX etc. is justified by the fact that it offers a free advanced toolbox for solving complex physical problems involving chemical reactions, turbulence and heat transfer with the advantage to be totally open and free, both in terms of source code and in its structure and hierarchical design [10].

4.1. Description of OpenFOAM (Open Field Operation and Manipulation) [12]:

Native development of OpenFOAM is done on a Linux / UNIX platform and specifically in the GCC (Gnu Compiler Collection) C++ compiler. To pre-process and solve cases, two ways are offered: use of the graphical user interface called FoamX or the Terminal. As direct access to OpenFOAM's source code is possible (text files in C), modifications of boundary conditions or input/output control are allowed by editing the files manually. The post-processing is done by ParaView.

4.2. Mesh (Fig. 5):

Although OpenFOAM has a mesh tool called BlockMesh exportation of other meshes is feasible. It is important to note that OpenFOAM is strictly a 3D code. To find an initial solution for a 2D axi-symmetric problem, the mesh must be 3D first with one cell thick and having no solution in Z- direction. We must ensure that the opening of the thickness of both sides between the Y-axis does not exceed the angle whose apex would be on the Y-axis and between 2.5° and 5° [2].

Quadrangular mesh is used due to the simple geometry of the 2D initial solution configuration while tetrahedron/hybrid mesh type is used due to the complex shape of the 3D geometry [19].

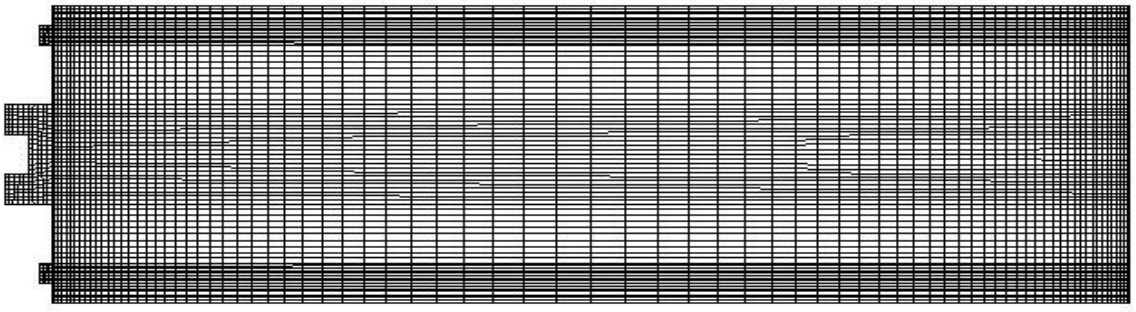

Fig. 4: 2D initial solution mesh view

5. Turbulence and combustion modeling

5.1. Turbulence [8]

The DNS (Direct Numerical Simulation) is effective when simple academic problems occur otherwise it would be numerically expensive as it can be seen in our case because the phenomena and configurations are complex. The advantage of LES (Large Eddy Simulation) is to combine modeling and direct calculation but the computation of its pre-processor and solver costs a lot. Another problem related to LES is that their coupling with other models is not yet mature in OpenFOAM. Taking in account all those points RANS (Reynolds Averaged Navier-Stokes) remains the only one approach more accessible to use in our work. The model chosen is k-ε standard because of its robustness, accuracy, low cost and rich documentation. Its weakness in walls zone can be offset by the Standard Model Wall Function (SWF).

5.2. Combustion [2]

For combustion gas, there are three types of solvers all operating in unsteady state: reactingFoam [10], Xoodles and XiFoam. Only reactingFoam models the non-premixed turbulent combustion. The concept it uses for the chemical species is the PaSR (Partially Stirred Reactor) which is a modified version of the EDC (Eddy Dissipation Concept) where the chemical time scale is handled differently.

- Expression of Air-Fuel reaction mechanism:

$$C_{19}H_{30} + 26.5O_2 \rightarrow 19CO_2 + 15H_2O \quad (17)$$

- Expression of the reaction rate constant according to Arrhenius kinetic model:

$$k(T) = AT^b \exp\left(-\frac{E_A}{R_u T}\right) \quad (18)$$

Where EA is the activation energy ($1.256x10^8$J/kg mol) and A is the pre-exponential factor ($2.587x10^9$).

The equation (14) was originally made for laminar case. If we want to adapt it to turbulent case, just define the mixture rate by the ratio:

$$turb_{mix} = \varepsilon / k \tag{19}$$

NB: the reaction mechanism is imported from Chemkin (software tool for solving complex chemical kinetics problems).

- ReactingFoam Code:
  1. Calculate chemical reaction based on turbulent and chemical timescales;
  2. Calculate of the density;
  3. Calculate velocity/pressure fields;
  4. Read species and feed them to the chemistry solver using Chemkin table;
  5. Calculate the temperature from the chemical reactions enthalpy lookup;
  6. Calculate the pressure field using PISO;
  7. Correct the turbulence (pressure-corrector);
  8. Update the density from the temperature;
  9. Return to step 1.

6. Numerical resolution [10]

Discretisation method used by OpenFOAM is Finite Volume (FVM). Only transient models like reactingFoam need temporal discretisation.

6.1. Temporal discretisation

To avoid instability due to the simultaneous calculation of turbulence and combustion, the first solver to use is simpleFoam which is a steady-state incompressible turbulence model. This is done to calculate the cold flow which will be considered as our initial solution. Knowing that reactingFoam is an unsteady solver, the time step depends strongly on the Courant number *Cr*. This is possible only with the CFL (Courant Friedrichs Lewy) condition:

$$C_r = \frac{\bar{v}\Delta t}{\delta x} \tag{20}$$

If $0 < C_r \leq 0.5$, we have more stability and less speed.
If $1 > C_r \geq 0.5$, we have more speed and less stability.
In this case, Cr = 0.2.

6.2. Interpolation schemes:

- Pressure: limitedLinear 1 (second order bounded scheme);
- Velocity: limitedLinearV (TVD scheme recommended for swirl);
- Turbulence: upwind (first order bounded scheme);
- Species: upwind;
- Energy: upwind;
- Pressure-velocity coupling: PISO (Pressure Implicit with Splitting of Operators).

7. Results

7.1. Advantages of swirling secondary air configuration:

7.1.1. Tight confinement

The swirling flow affects the behavior of the flame because we are dealing with a tight confinement, in other words, the dimensions (ie, diameter) of the injector are not negligible compared to the chamber dimensions (Fig. 1 & 2) [13].

7.1.2. Decrease of unburned rate

From thermodynamic studies it has been shown that a small amount of trace species in the combustion products can have a great impact on the CO_2 capture, storage and transportation [18]. Now the mass fraction of fuel (mFf) at the outlet has almost decreased by an half as can confirm the values and graph below (Fig. 5):

- mF_f (without swirl)= ±0.1057;
- *mFf* (with coflow: *S*=0) = ±0.0478;
- mF_f (with swirl: *S*=0.3)= ±0.0478.

This will enable a better control of pollution due to CO_2 production.

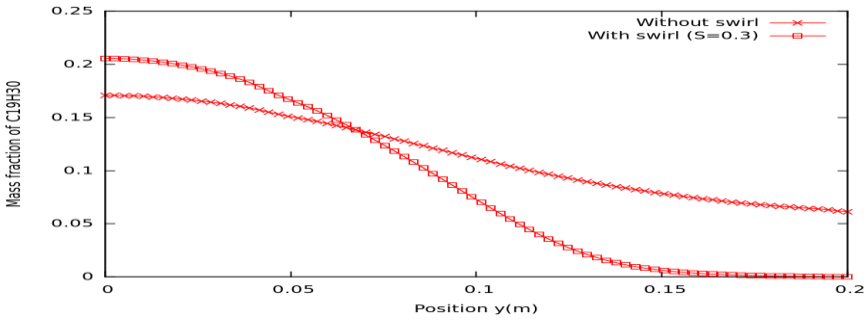

Fig. 5: Outlet mass fraction of $C_{19}H_{30}$

7.1.3. Better protection of walls

Temperature decreases considerably near the walls (Fig. 6). This fall ΔT is inversely proportional to S. This is verified through values of transversal temperature differences observed when *S*=0 or *S*=0.3 (Fig. 7 & 8).

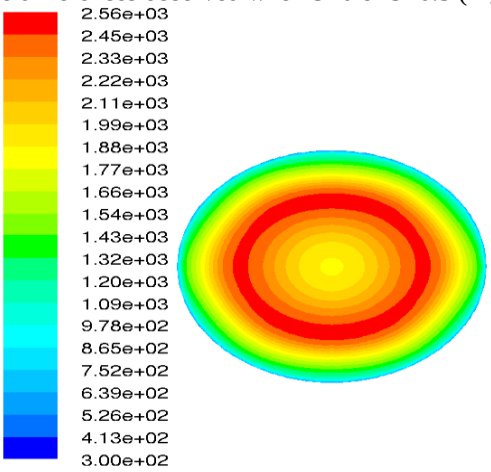

Fig. 6: Radial evolution of temperature contours

- For internal transversal temperature: if *S* = 0.3: $\Delta T_{swirl} = T - T_{swirl} = 1150°C$ (Fig. 7)

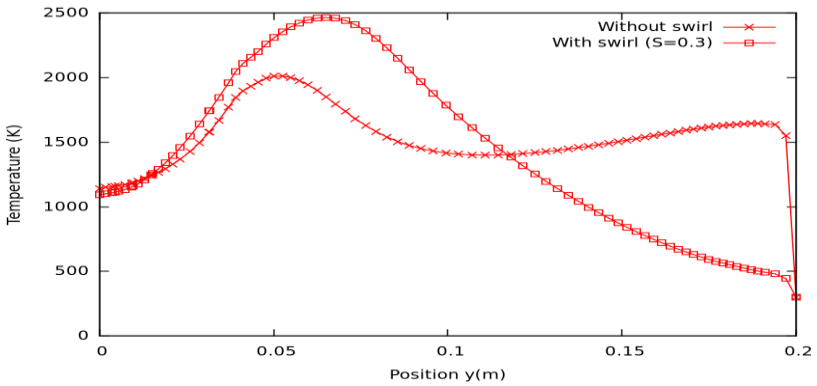

Fig. 7: Internal transversal temperature (x=0, z=0.52)

- For outlet transversal temperature: if *S* = 0.3: $\Delta T_{swirl} = T - T_{swirl} = 650°C$ (Fig. 8)

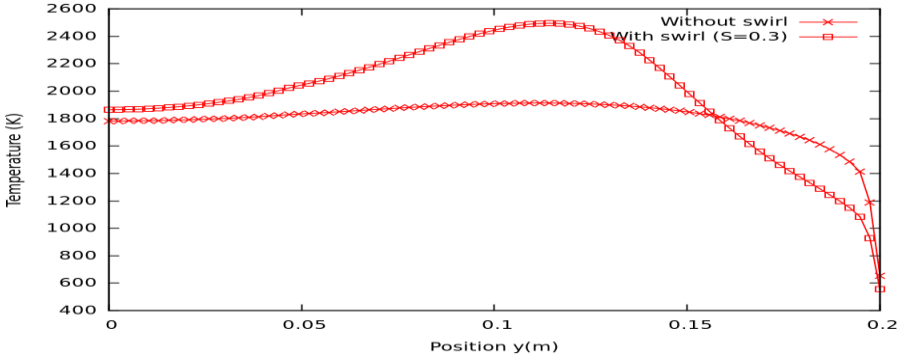

Fig. 8: Outlet transversal temperature

7.1.4. Stabilization of combustion:

In practical combustion chambers the mixing time for the fuel and oxidizer is typically larger than the chemical reaction time [18].

Stabilization of combustion is done by increasing the residence time of the flame and creating recirculation in the reaction zone. The effect produced is to favor the mixture and give to the flame a more compact form [13] (Fig. 9, 10, 11, 12 & 13). The axial evolution of swirling temperature profile is almost linear (Fig. 11). It means that swirl configuration provides better and easiest control of temperature in flow direction.

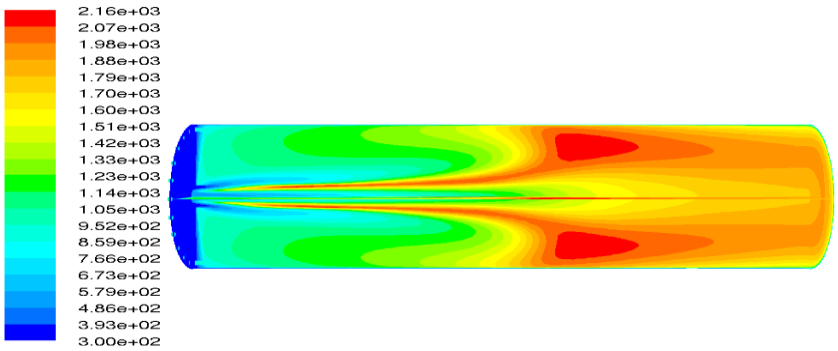

Fig. 9: Temperature contours without swirl

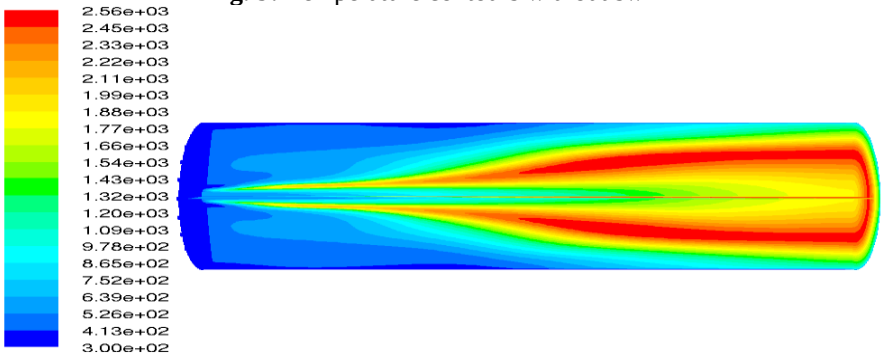

Fig. 10: Temperature contours with swirl

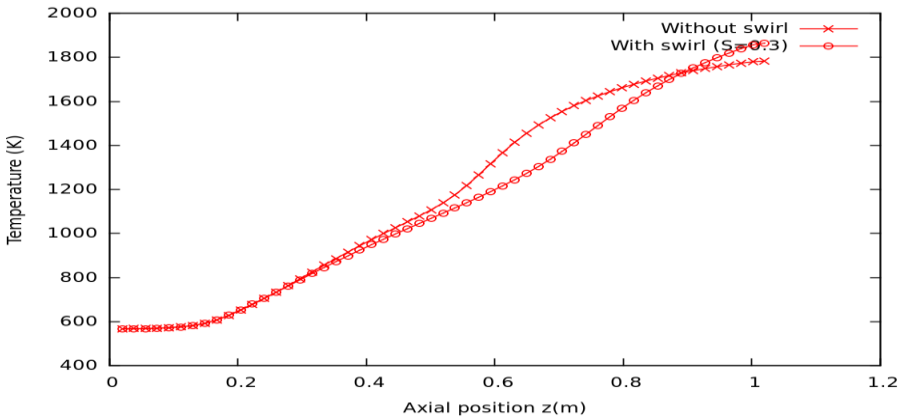

Fig. 11: Axial temperature evolution

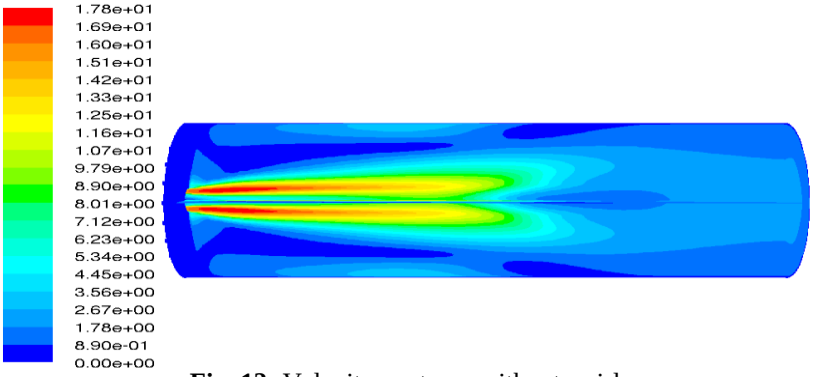

Fig. 12: Velocity contours without swirl

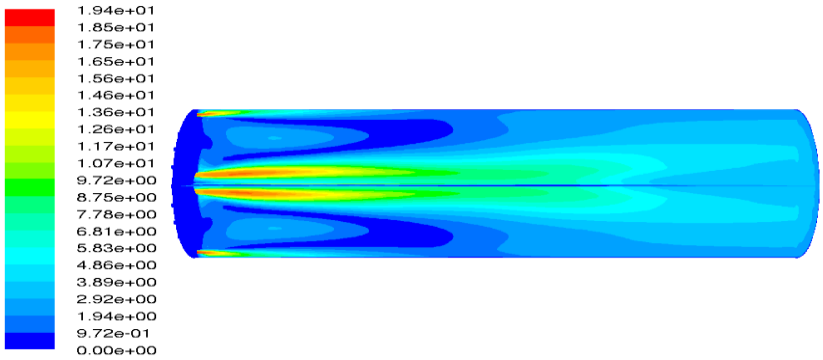

Fig. 13: Velocity contours with swirl

7.1.5. Reduction of the CO_2 formation:

Values and graphs of mF(CO_2) below (Fig. 14 & 15) reveal a decrease of the outlet CO_2 mass fraction in the case of intense swirl:

- Without swirl, mF(CO_2) = ± 0.1893;
- With coflow (S=0), mF$(CO_2)_{coflow}$= ± 0.1677;
- With swirl (S=0.6), mF$(CO_2)_{swirl}$ = ± 0.1637.

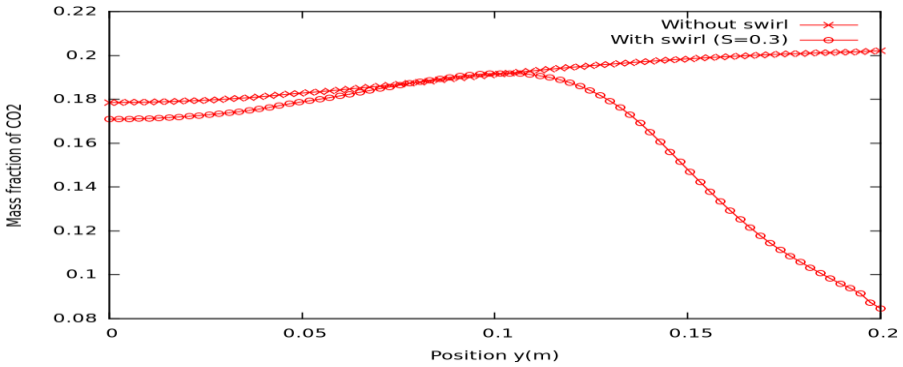

Fig. 14: Outlet mass fraction of CO_2

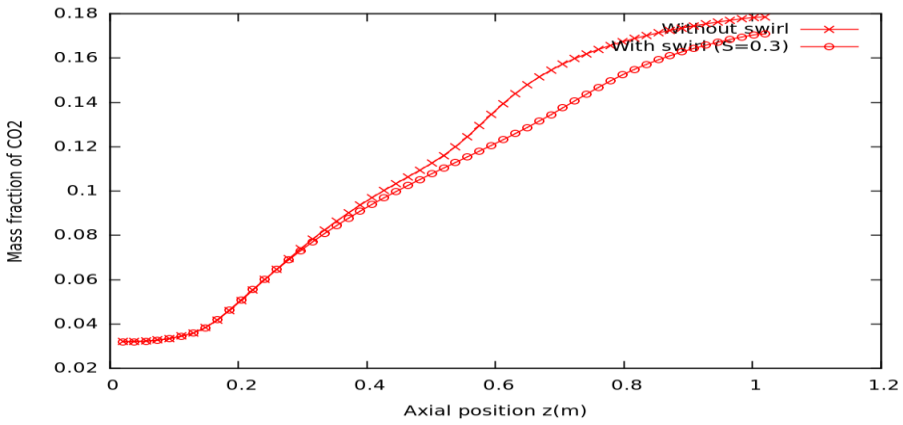

Fig. 15: Axial mass fraction of CO_2

7.2. Disadvantages of swirling secondary air configuration:

7.2.1. Rise of outlet temperature

Calculation of the mass-weighted average value of temperature at outlet gives:

$$\overline{T} = \frac{\int T\rho\vec{V}d\vec{A}}{\int \rho\vec{V}d\vec{A}} \qquad (21)$$

- Without swirl, $\overline{T}$ = ±1827K;
- With coflow (S=0), $\overline{T}_{coflow}$ = = ±1934K ;
- With swirl (S=0.6), $\overline{T}_{swirl}$ = = ±1879K.

7.2.2. Amplification of the swirl promotes NO formation

The same observation was made on a small scale by Vauchelles [16]. After 3 test cases (S=0.3; S=0.5; S=0.7) of swirling secondary air injection to a combustion chamber of gas turbine engine, he asserts that the reduction of CO_2 emissions means better combustion and thus a rise of temperature controlling NO.

To reach this conclusion, the following two approaches can be used:

- Calculation of *NO* concentration (ppm) in the gas mixture:

NO ppm is computed from the following equation:

$$NOppm = \frac{MF(NO)X10^6}{1 - MF(H_2O)} \tag{22}$$

Where:

$$MF(NO) = \frac{mF(NO)XMW(mixture)}{30} \tag{23}$$

After calculation, it can be seen through the values and graphs of *MW(NO)* below (Fig. 16 & 17) that the swirl promotes the production of NO.

- Without swirl, *MW(NO)* ≈ 1019 ppm;
- With coflow *(S=0)*, *MW(NO)coflow* ≈ 2933 ppm;
- With swirl *(S=0.6)*, *MW(NO)swirl* ≈ 3152 ppm.

- Estimation of average mass fraction of outgoing NO:

The mass fraction of outgoing NO experienced a sharp increase with the intensification of the swirl.

- Without swirl, *mF(NO)* ≈ 0.0011 ;
- With coflow (S=0), *mF(NO)* ≈ 0.0092 ;
- With swirl (S=0.6), *mF(NO)* ≈ 0.0091.

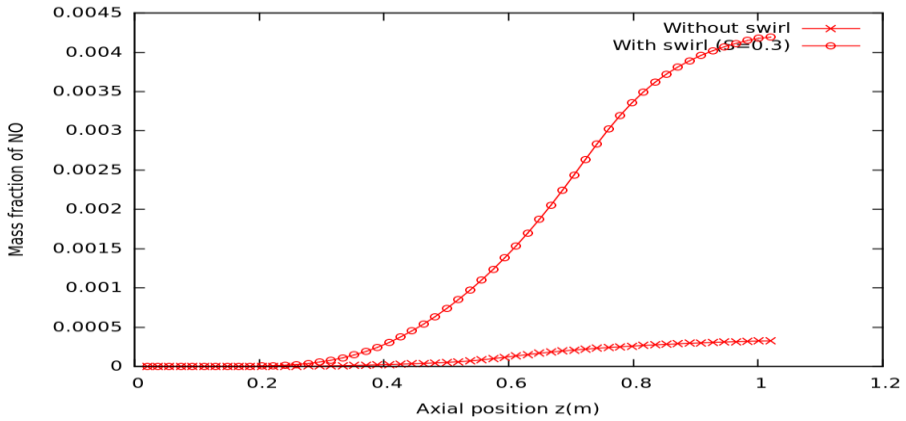

Fig. 16: Axial mass fraction of NO

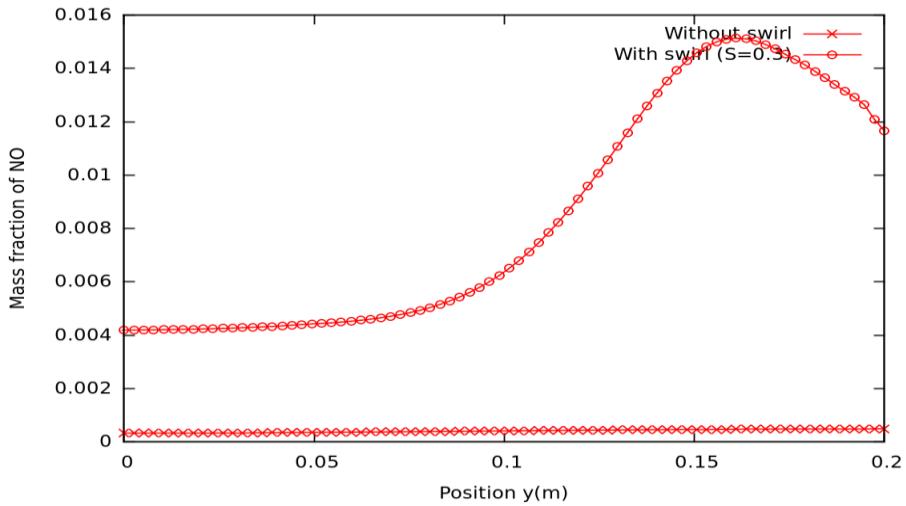

Fig. 17: Outlet mass fraction of NO

8. Conclusions and perspective

To better understand the potential role of a secondary air swirling flow in a turbulent non-premixed combustion chamber two test cases situations are considered : a pure axial jet called "coflow" (with S= 0) and an weak swirl jet (with S=0.3) characterized by the presence of an IRZ (Internal Recirculation Zone). Non-premixed flames can be quenched by lowering the temperatures of the oxidizer stream, or by increasing the flow strain rate (equivalently scalar dissipation rate) [18]. In the first case there is a possible risk of blowing phenomenon for the secondary air flow strain rate is increased. As it is known the blow tends to get rid of the IRZ pushing the flame to hanging or extinction. In the last case [15] a flashback to the injector's tube can occur and lead to a suspension of the flame. Flashback occurs when the gas velocity becomes lower than the burning velocity due to flame propagation within boundary layer, core flow or because of combustion instabilities [22]. Flashback in swirl burners [23] can be caused by a phenomena termed combustion induced vortex breakdown (CIVB) due to rapid expansion at the burner exit creating a recirculation zone which acts as a flame holder: the breakdown of this structure can occur due to flow perturbations and chemical reaction effects causing the CRZ (Central Recirculation Zone) and hence flame to propagate upstream into the premixing zone [23, 24].

Neither of these two phenomena was observed because of the good tight confinement between combustion chamber and swirling air injectors. This led us to introduce confidently discussion about the flame stability based on the influence of number of Swirl (*S*). Studies will be extended in the next paper to deal with greater values of *S*.

About the combustion intensity, we noticed simultaneously an increase of NO formation and a decreased of CO_2 production. We know that the two gases are the leading pollutants in combustion sites [7]. This is justified by the fact that the main reaction mechanism involved for NO is that of Zeldovich (1946) which is essentially thermal as it is generated by the rise of the activation temperature in a reaction zone such as an oxidizing environment [15]. This observation is quite normal for in non-premixed condition, fuel is injected in shear region formed near to the zero stream line boundary and recirculation region which provides the low velocity region for flame stabilization with the evolution of high temperatures from the flame. For flames operating in diffusion mode, the reaction zone is stabilized to result in large temperature gradients and hot-spot regions in the entire combustion chamber that result in high NO levels [9] from the combustion of fuels. NO emission increased due to the accelerated chemical kinetics of the combustion process [19]. Concerning CO_2 production, it is possible to reduce more by increasing the inlet air temperature but this will result in increasing the flame temperature which in its turn will increase the production of NO [19]. Another solution to explore about CO_2 production can be the elevation of pressure into the combustor. As said Ahmed E.E. Khalil and al. [19] this will promote the combustion kinetics to enhance the combustion reactions. At low equivalence ratios, increase in pressure diminishes CO by accelerating the rate of conversion of CO into CO_2. At high equivalence ratios, increase in combustion pressure reduces CO emissions, albeit to a lesser extent, by suppressing chemical dissociation. So in one aspect high pressures are beneficial, but on the other hand, high pressure also accelerated NOx formation leading to higher NO emissions [19].

The future work will be to control temperature so as to expect a good balance between reducing pollution and improving combustion. Moreover, the protection of walls remains a priority. For complete study, it will be better to couple the influence of temperature with the humidity effects near walls by means of transversal evolution of H_2O mass fraction.

To assess the stability of reactingFoam, the role of convection schemes in the solution was investigated. That is the reason why we used successively upwind and limitedLinear to compute the energy and species. The result was the same but instability (represented by "wiggles") occurred in the temperature profile when we tried QUICK scheme. Versteeg and Malalasekera [17] have showed that this is due to the QUICK schemes nature, which has a tendency to produce over-shoots and under-shoots in the results and thus producing the obtained "wiggles".

References

1. Albouze, G., Simulation aux grandes échelles des écoulements réactifs non-prémélangés, Ph.D. thesis, Université de Toulouse, 2009.
2. C. Andersen, E. L. Nielsen Niels, Numerical investigation of a BFR using OpenFOAM, Project of Fluids and Combustion Engineering (2008) p.18.
3. Acta Physicochim, "Thermal NO Mechanism ou Zeldovich Mechanism", 1946, 21, 577.
4. R. W. Bilger, International workshop on measurement and computation of Turbulent Non-premixed Flames: References on Swirl Flames, Updated November 2005.
5. Criner, K., Stabilisation de flammes de diffusion turbulentes assistée par plasma hors-équilibre et par champ électrique, Ph.D. thesis, Université de Rouen, 2008.
6. D. Elkaïm, M. Agouzoul and R. Camarero, "A Numerical Solution for Reacting and Non Reacting Flow", Lectures Notes in Physics, Edited by Dervieux A. and Larouturou B., Springer-Verlag, 1989.
7. Ferrand, L., Modélisation et expérimentation des fours de réchauffage sidérurgiques équipés de brûleurs régénératifs à oxydation sans Flamme, Ph.D. thesis, Ecole des Mines de Paris, 2003.
8. FLUENT Inc., Fluent 5.5 User's guide, October 2000.
9. Gupta, A. K. Lilley, D.G. Syred, N., Swirl Flows, Gordon & Breach Science Pub, 1984.
10. Lundström, A. reactingFoam Tutorial, Chalmers University of Technology, 2008.

11. W. Meier, O. Keck, B. Noll, O. Kunz, & W. Stricker, "Investigations in the TECFLAM Swirling Diffusion Flame: Laser Raman Measurements and CFD Calculations", Appl. Phys. (2000) B71:725-731.
12. OpenCFD, OpenFOAM – User Guide, 1st August 2007, Version 1.4.1.
13. Poireault, B. Mécanisme de combustion dans un brûleur méthane-air de type swirl (40kW): influence de l'intensité de la rotation. Ph.D. thesis, Université de Poitiers, 1997.
14. T. Raffak, M. Agouzoul, M. Mabsate, A. Chik & A. Alouani, "Recent Patent and Modeling of Phosphate Rotary Dryer", Recent Patents on Engineering, June, 2008, Volume 2, Issue 2, pp.132-141.
15. Taupin, B. Etude de la combustion turbulente à faible richesse haute température et haute pression, Ph.D. thesis, Institut national des sciences appliquées de Rouen (2003) pp. 24-27.
16. Vauchelles, D., Etude de la stabilité et des émissions polluantes des flammes turbulentes de prémélange pauvre à haute pression appliquées aux turbines à gaz, Ph.D. thesis, INSA-Rouen, 2004.
17. Versteeg, H. K. Malalasekera, W., An introduction to computational fuid dynamics, The finite volume method, second ed. Pearson Education Limited, 2007.
18. C.Y. Liu, G. Chen, N. Sipöcz, M. Assadi, X.S. Bai, Characteristics of oxy-fuel combustion in gas turbines, Applied Energy 89 (2012) 387–394.
19. Ahmed E.E. Khalil, Ashwani K. Gupta, Distributed swirl combustion for gas turbine application, Applied Energy 88 (2011) 4898–4907.
20. Harun Mohamed Ismail, Hoon Kiat Ng, Suyin Gan, Evaluation of non-premixed combustion and fuel spray models for in-cylinder diesel engine simulation, Applied Energy 90 (2012) 271–279.
21. J. Ward, M. Mahmood, Heat transfer from a turbulent, swirling impinging jet, Proceedings of the 7th International Heat Transfer Conference 3 (1982) 401-407.
22. Sankaran R, Hawkes ER, Chen JH, Lu T, Law CK. Direct numerical simulations of turbulent lean premixed combustion. J Phys 2006; 46:38–42.
23. Fritz J, Kroner M, Sattelmayer T. Flashback in a swirl burner with cylindrical premixing zone. J Eng Gas Turb Power 2004; 126(2):276–83.
24. Kroner M, Fritz J, Sattelmayer T. Flashback limits for combustion induced vortex breakdown in a swirl burner. J Eng Gas Turb Power 2003; 125(3):693–700.
25. CORIA, Actes de la Sixième Conférence Francophone en Recherche d'Information et Applications, Hyères, France, 2009.